

Article

Investigating the Impacts of Biochar Amendment and Soil Compaction on Unsaturated Hydraulic Properties of Silty Sand

Zhongkui Chen ¹, Viroon Kamchoom ^{2,*} , Rui Chen ³ and Lapyote Prasittisopin ⁴ ¹ Shenzhen Yanzhi Science and Technology Co., Ltd., Shenzhen 518101, China; brucechenyzte@163.com² Excellent Centre for Green and Sustainable Infrastructure, School of Engineering, King Mongkut's Institute of Technology Ladkrabang, Bangkok 10520, Thailand³ School of Civil and Environmental Engineering, Harbin Institute of Technology Shenzhen, Shenzhen 518055, China; cechenrui@hit.edu.cn⁴ Department of Architecture, Faculty of Architecture, Chulalongkorn University, Phaya Thai Road, Pathumwan, Bangkok 10330, Thailand; lapyote.p@chula.ac.th

* Correspondence: viroon.ka@kmitl.ac.th

Abstract: The application of biochar as an environmentally friendly additive for agricultural soils has recently gained significant attention. However, the influence of biochar addition on unsaturated hydraulic behavior at high suction ranges (i.e., exceeding 100 kPa) remains largely understudied. This study investigates the impact of biochar addition on the unsaturated hydraulic properties of biochar amended soil (BAS). The effects of biochar content, particle size, and soil compaction on the unsaturated hydraulic properties of BAS were also considered. Peanut shell biochar was utilized in this investigation and was amended into a compacted silty sand with distinct particle size groups. Soil water retention curves and unsaturated permeability were measured through a series of evaporation tests. Results demonstrate that the impact of soil compaction on the unsaturated hydraulic properties of BAS diminishes at high suction range, regardless of biochar particle size and content. A high degree of compaction reduces the saturated permeability of BAS by minimising soil macropores. On the other hand, incorporating high biochar contents with fine particles into the soil enhances the reduction of unsaturated permeability and the improvement of water holding capacity, thereby making biochar an effective application in soil for sustainability of the agroecological environment.

Keywords: peanut shell biochar; compacted silty sand; evaporation method; soil water retention curve; unsaturated permeability



Citation: Chen, Z.; Kamchoom, V.; Chen, R.; Prasittisopin, L. Investigating the Impacts of Biochar Amendment and Soil Compaction on Unsaturated Hydraulic Properties of Silty Sand. *Agronomy* **2023**, *13*, 1845. <https://doi.org/10.3390/agronomy13071845>

Academic Editors: Roberto Mancinelli, Emanuele Radicetti and Ghulam Haider

Received: 29 May 2023
Revised: 28 June 2023
Accepted: 5 July 2023
Published: 13 July 2023



Copyright: © 2023 by the authors. Licensee MDPI, Basel, Switzerland. This article is an open access article distributed under the terms and conditions of the Creative Commons Attribution (CC BY) license (<https://creativecommons.org/licenses/by/4.0/>).

1. Introduction

The use of biochar is becoming increasingly popular as a means of addressing environmental concerns, particularly those related to climate change and eco-friendly practices in the agriculture and geoenvironmental sectors. The raw materials for biochar production are often derived from biomass waste, such as peanut husks, rice husks, and straw, which would otherwise be left to decompose and release greenhouse gases into the atmosphere [1]. The preparation process for biochar is also relatively simple, making it a cost-effective green solution for reducing carbon emissions [2–4]. In addition to its carbon sequestration capabilities, biochar also has numerous benefits for soil health and crop productivity. Its high adsorption capacity and porosity allow it to improve soil fertility, reduce soil water infiltration, and increase crop yields [5–8]. Biochar has also been shown to be effective in reducing landfill gas emissions and remediating contaminated soil [9–11].

Given the fact that climate change is already causing significant changes in precipitation patterns with more frequent and intense droughts and rainfall events, this can result in a severe shortage of water available to plants, which can impact their growth and productivity [12,13]. Additionally, it can also lead to increased cracks, which can contribute to soil erosion and instability [11,14]. Biochar's ability to modify the water seepage

and retention in biochar-amended soil (BAS) is of critical importance as water is a vital component for the transport of nutrients to plants and the survival of the soil microbial community [15–17]. Consequently, it is imperative to further investigate how biochar application impacts the permeability and water retention properties of the BAS. Previous studies have explored the influence of biochar on soil water retention both in laboratory and field conditions [6,18,19]. For instance, Sun and Lu [20] found that biochar addition significantly increases the available water content in soil, thereby improving its water retention capacity. Similar results were obtained in subsequent experiments, which demonstrated that biochar application improved soil water retention through an increase in total pore volume [21,22]. Omondi et al. [23] suggested that biochar addition significantly enhanced water retention and permeability of BAS, regardless of the feedstock, pyrolysis temperature, or soil type used. Edeh et al. [24] further showed that the effect of biochar on soil permeability varied depending on the grain size of the soil, with the saturated permeability of fine-grained soil increasing by 39.3% on average and the saturated permeability of coarse-grained soil decreasing by 61.8%.

In the fields of agricultural and environmental geotechnical engineering, the unsaturated hydraulic properties of soil, including water retention and permeability, play a crucial role in evaluating the seepage of embankments, subgrades, and landfill covers. These properties are highly related to the soil pore size and structure [25,26]. However, some studies have reported conflicting results, with either a decrease in or no significant effect of biochar on water retention and permeability [6,18,27]. To resolve this discrepancy, Trifunovic et al. [28] investigated the hydraulic properties of biochar-amended pure sand and discovered that an increase in biochar concentration decreased the unsaturated permeability of BAS, regardless of the biochar particle size. Despite these findings, the study was limited to soil suction values of 100 kPa, which only covered the available water use for crops or plants in agricultural fields. In engineering, higher soil suction is crucial for assessing the stability of green slopes and the prevention of water percolation in landfill covers [29–32]. However, research on the unsaturated properties of highly compacted BAS at suction values higher than 100 kPa is limited. Given the pressing need to mitigate the effects of climate change, it is crucial to continue investigating and comprehending the impact of biochar application on soil permeability and water retention properties.

The degree of compaction can be a crucial factor that contributes to the discrepancy in the results of previous studies regarding the impact of biochar on soil properties. Compaction can significantly influence the behavior of BAS and its hydraulic properties, which have implications for various engineering and agricultural applications. However, the effect of biochar on the hydraulic properties of soil may vary depending on the degree of compaction. Hussain et al. [33] reported that the impact of biochar on soil hydraulic properties might differ between densely compacted and agricultural soils. Therefore, it is imperative to understand the unsaturated hydraulic performance of BAS in both types of soil, especially under a wide range of soil suction, which reflects the available water use. According to previous studies [11,34,35], a higher degree of compaction is generally required for geoen지니어ed systems such as landfill covers. On the other hand, agricultural protocols advocate for less compaction, as it benefits soil aeration and plant growth. Understanding the unsaturated hydraulic behavior of BAS is essential for optimizing the use of biochar as an agricultural amendment and for the sustainable design of landfill covers.

The primary objectives of this study are to examine the soil water retention of BAS with varying biochar contents and to assess the impact of soil compaction on its permeability (saturated and unsaturated). The specific hypotheses addressed in this study are as follows:

1. Higher biochar contents will lead to increased water retention and improved soil pore structure, resulting in enhanced water-holding capacity;
2. The finer biochar particles will exhibit greater improvements in soil water holding capacity and permeability due to their ability to enhance soil porosity and alter pore size distribution;

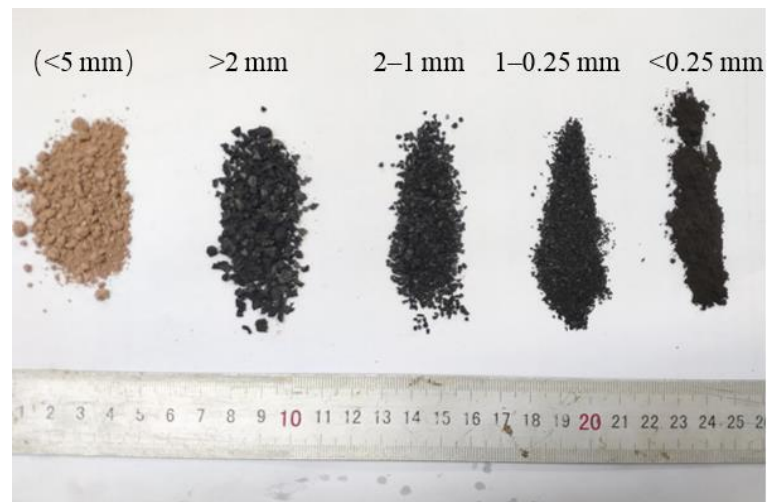
3. The soil compaction levels will interact with biochar additions, leading to varied impacts on water retention and permeability. Different responses may be observed between agricultural soils and densely compacted soils, highlighting the importance of considering compaction effects on hydraulic behavior.

To achieve these objectives, a series of experiments were performed on compacted, completely decomposed granite (CDG) which was clarified as a silty sand, amended with different particle sizes of peanut shell biochar. The water retention curve and unsaturated permeability function of BAS were measured, and the saturated permeability was determined through the use of falling head tests in the geotechnical laboratory of Harbin Institute of Technology Shenzhen in China. The outcome can be a basis for future research on the optimisation of biochar content under different levels of compaction. The compaction levels of 80% and 90% were chosen to specifically address the challenges associated with agriculture and landfill applications. Higher compaction degrees are problematic in agriculture, while lower compaction degrees pose challenges in landfill settings. The study aimed to investigate the impact of biochar addition on these specific compaction levels to provide insights and potential solutions for each application. The findings will contribute to the development of agricultural practices that can improve soil fertility and water retention and also enhance sustainable geoenvironmental systems that can minimize soil permeability and enhance the integrity of the earthen structure, especially under extreme climate conditions.

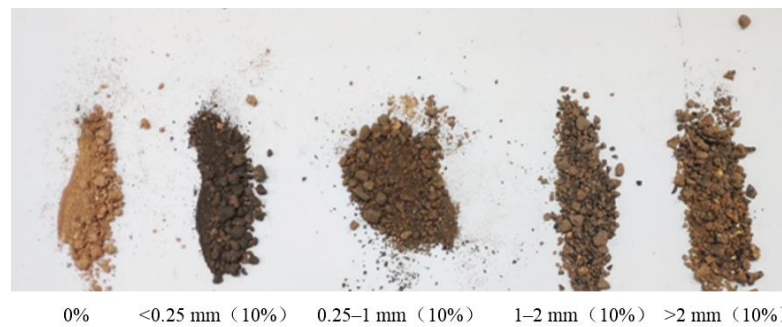
2. Materials and Methods

2.1. Biochar and Soil

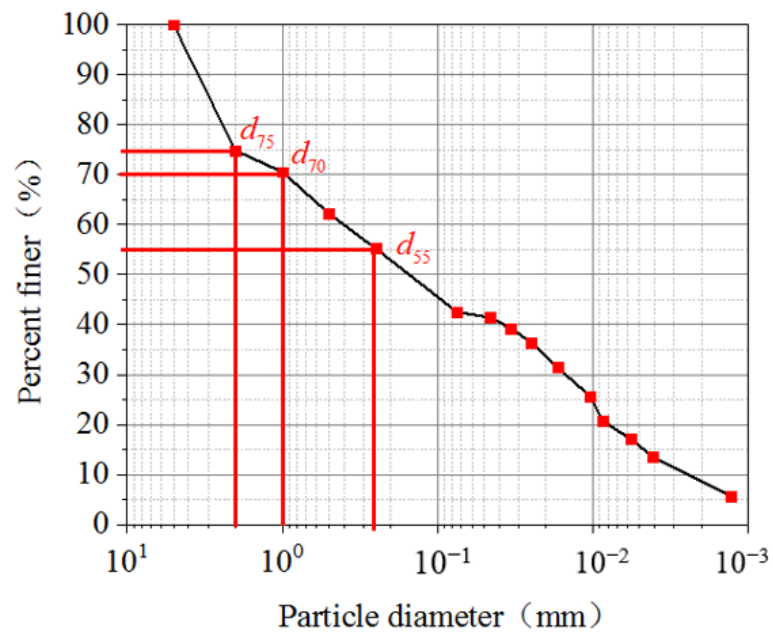
The biochar used in the experiments was sourced from a recycled material company in China. The biochar was produced from agricultural waste, specifically peanut shell, using the slow pyrolysis process. The biochar was then subjected to particle size analysis through sieving using three sieves with mesh sizes of 0.25 mm, 1 mm, and 2 mm. The result of this analysis formed four particle size groups, which were <0.25 mm, 0.25–1 mm, 1–2 mm, and >2 mm. To minimize the impact of the original moisture content on the biochar, all the biochar samples used in the experiments were oven dried at 105 °C for 24 h. The soil used in the experiments was CDG collected from a construction site in Shenzhen, China. This soil type is commonly used as construction material in many countries, including Thailand and China. The soil was analyzed according to the Unified Soil Classification System, which revealed that it consisted of 57.4% sand, 27.6% silt, and 15.0% clay. The soil was classified as SM (silty sand). The mineral compound concentration for the soil is quartz (46%), kaolin (43%), illite (6%), and gibbsite (5%). The soil organic matter content is 4.4–4.8%. The index properties of the soil were reported in Chen et al. [32]. The particle size distribution of the soil, as well as a photograph of the testing materials, can be seen in Figure 1. As shown in Figure 1c, the three biochar particle sizes corresponded to the d_{55} , d_{70} , and d_{75} of the soil grain size, respectively. The significance of particle size in biochar has a direct impact on its efficacy as a soil amendment. The objective of utilizing biochar is to enhance its surface area for optimal interaction with the soil, as this interaction is essential for the provision of benefits such as improved soil fertility and structure, and increased water retention capacity [36,37]. It is thus expected to select a particle size for biochar that is comparable to the mean size of soil grains. This correlation between particle size and soil grain size facilitates the intermixing of biochar and soil, thereby increasing the contact between the two [38,39]. This increased contact between the biochar and soil allows for greater exchange of nutrients, water, and other important substances, leading to a more productive and healthy soil environment.



(a)



(b)



(c)

Figure 1. Testing materials: (a) soil and biochar with different biochar particle sizes; (b) mixture of soil and biochar (10% *w/w*) with different biochar particle sizes; (c) particle size distribution of the CDG soil.

2.2. Physical Properties of the Testing Materials

The Fourier Transform Infrared Spectrometer (FTIR) model (Thermo Fei IS90) was employed to conduct infrared characterization on the biochar sample. As depicted in Figure 2, the infrared spectrum of the biochar displayed various peaks at different wave numbers, each representing a specific chemical bond or functional group within the sample, as determined through comparison with standard compound spectra [40]. This allowed for the identification of the functional groups present in the biochar. The figure illustrates the presence of significant absorption peaks at wave numbers 3440 cm^{-1} , 2923 cm^{-1} , 1384 cm^{-1} , 1628 cm^{-1} , and 1031 cm^{-1} . The broad peak at 3440 cm^{-1} corresponds to the hydroxyl-O-H stretching vibration, which is indicative of the presence of hydroxyl groups. The peak at 2923 cm^{-1} is attributed to the C-H stretching vibration of C-H bonds, while the peak at 1384 cm^{-1} is assigned to the C-H bending vibration. The peak at 1628 cm^{-1} represents the stretching vibration of carbonyl C=O, and the peak at 1031 cm^{-1} corresponds to the C-O stretching of the carbon-oxygen bond. These results indicate the presence of abundant functional groups on the surface of the biochar, including hydrophilic groups such as hydroxyl (O-H), suggesting that the biochar used in the experiments is hydrophilic in nature.

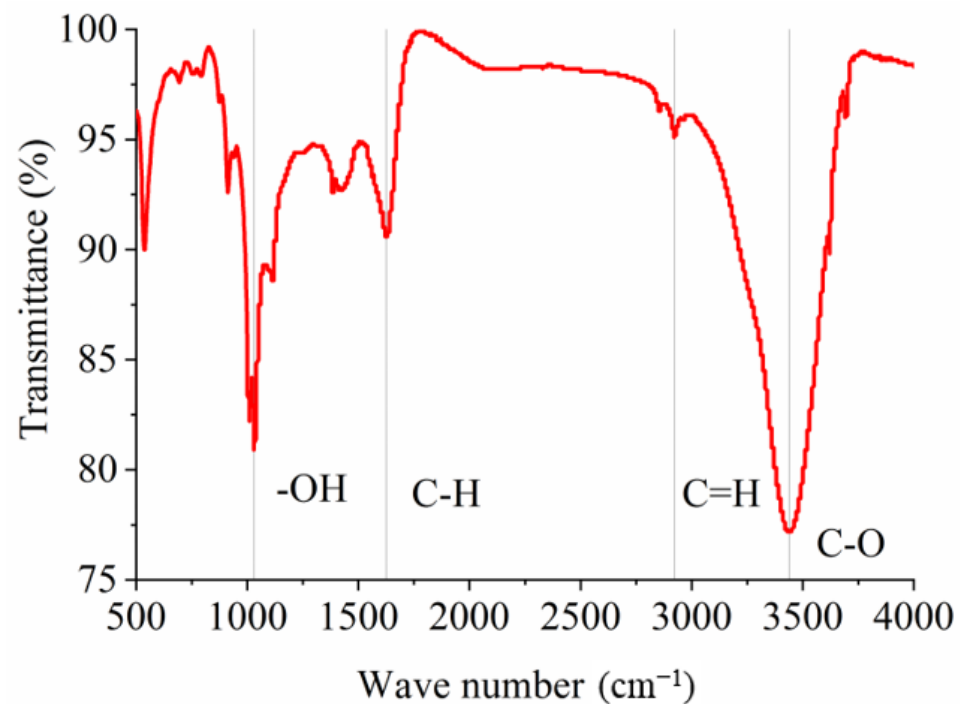


Figure 2. Infrared spectra of the biochar.

2.3. Measurement of Saturated Water Permeability of BAS

The saturated permeability of a BAS material was determined through the application of the falling head method in the geotechnical laboratory of Harbin Institute of Technology Shenzhen in China, in accordance with the guidelines outlined in the standard GB/T 50123-2019. The measurement was carried out using a permeameter (Model TST-55, Nanjing Soil Instruments Factory, Nanjing, China), which was specifically designed for this purpose. Before the test, the top and bottom of each soil specimen was covered with a piece of filter paper, and a porous stone was positioned at each end to prevent soil loss. The samples were then subjected to the vacuum saturation method described in the ASTM C1202 [41] standard. This involved placing the sample in a vacuum container for 3 h without water, followed by the introduction of de-aerated water into the container until the samples

were fully submerged for 8 h. The saturated hydraulic conductivity was calculated using Equation (1) [42]:

$$K_{sat} = 2.3 \frac{aL}{A(t_2 - t_1)} \lg \frac{h_1}{h_2} \quad (1)$$

where K_{sat} is the saturated permeability; a is the cross-section area of the falling head pipe (cm^2); A is the cross-section area of the specimen (cm^2); 2.3 is the scaling factor between \ln and \lg ; L is specimen height (cm); t_1 and t_2 is start and end time of the reading head (s); and h_1 and h_2 denote starting and ending hydraulic head difference (cm).

2.4. Measurement of Soil Water Retention Curve and Unsaturated Permeability

Evaporation tests were performed to determine the soil water retention curve (SWRC) and unsaturated permeability in the geotechnical laboratory of Harbin Institute of Technology Shenzhen in China, utilizing the simplified evaporation method. This method offers two significant benefits over conventional techniques, as highlighted by Schindler et al. [43], including a shorter testing duration and the simultaneous measurement of both the SWRC and unsaturated permeability function. The SWRC represents the relationship between soil moisture content and matric suction and typically encompasses both the drying and wetting curves. In this study, the drying curve of the SWRC was evaluated through the evaporation tests, with soil matric suction and water content being measured using tensiometers and an electronic balance, respectively.

The testing device used for the evaporation tests in this study is depicted in Figure 3. This device is capable of simultaneously obtaining both the SWRC and unsaturated permeability function, as reported by Chen et al. [44]. To perform the experiment, a mixture of peanut shell biochar and CDG soil was prepared, and water was added at its optimum water content to form the BAS mixture. Subsequently, a soil sample was compacted in a cylindrical plexiglass column with an inner diameter of 65 mm, an outer diameter of 70 mm, and a height of 95 mm (Figure 3). The compaction process was conducted in 5 sub-layers, with each layer being 19 mm thick, and the surface between the consecutive sublayers was carefully scratched to ensure good contact. The BAS was compacted to reach a target dry density, which was either 80% (the dry density is 1.328 g/cm^3) or 90% (the dry density is 1.494 g/cm^3) degree of compaction. After the soil samples were compacted, the soil cylinder was saturated in accordance with ASTM C1202 [41]. The cylinder was wrapped in a membrane before being placed in a vacuum chamber with de-aired water. The bottom of the soil cylinder was then sealed, and two holes were drilled in the side of the soil sample, with a vertical spacing of 55 mm between the two holes. To measure a wider range of PWP, high-capacity tensiometers (Model YZ-500, Shenzhen Yanzhi Science and Technology Co., Ltd, Shenzhen, China) were installed in each hole. These tensiometers are capable of measuring soil suction directly from 0 to 500 kPa with an accuracy of 2 kPa [45]. In order to reduce the error caused by cable interruption during measurement, a wireless data logger was used along with an electronic balance with a precision of 0.1 g. The tensiometer cables were connected to a signal transmitter, and the data were transmitted to the data logger via WiFi.

The evaporation was carried out under relatively constant temperature and humidity conditions in the laboratory. During the experiment, the readings from the upper and lower tensiometer, as well as the water loss changes of the soil samples, were automatically collected in real-time by the wireless data logger and the electronic balance, respectively. The soil suction was measured by the two tensiometers, and the water content was obtained from the water loss of the soil samples during the experiments. The average suction value of the two tensiometer readings was considered to form the SWRC, and the measured SWRC was fitted using the Van Genuchten (VG) model [46] (see Equation (2)). The unsaturated permeability function of the BAS was obtained following Equations (3) and (4) [43].

$$\theta = \theta_r + \frac{(\theta_s - \theta_r)}{[1 + (\alpha\psi)^n]^m} \quad (2)$$

where θ is the volumetric water content (%); ψ is the soil suction; θ_r and θ_s are the residual and saturated volumetric water content; α is an empirical scale parameter; n is the curve shape factor which controls the slope of the SWRC; and m is an empirical shape factor related to n by $m = 1 - 1/n$.

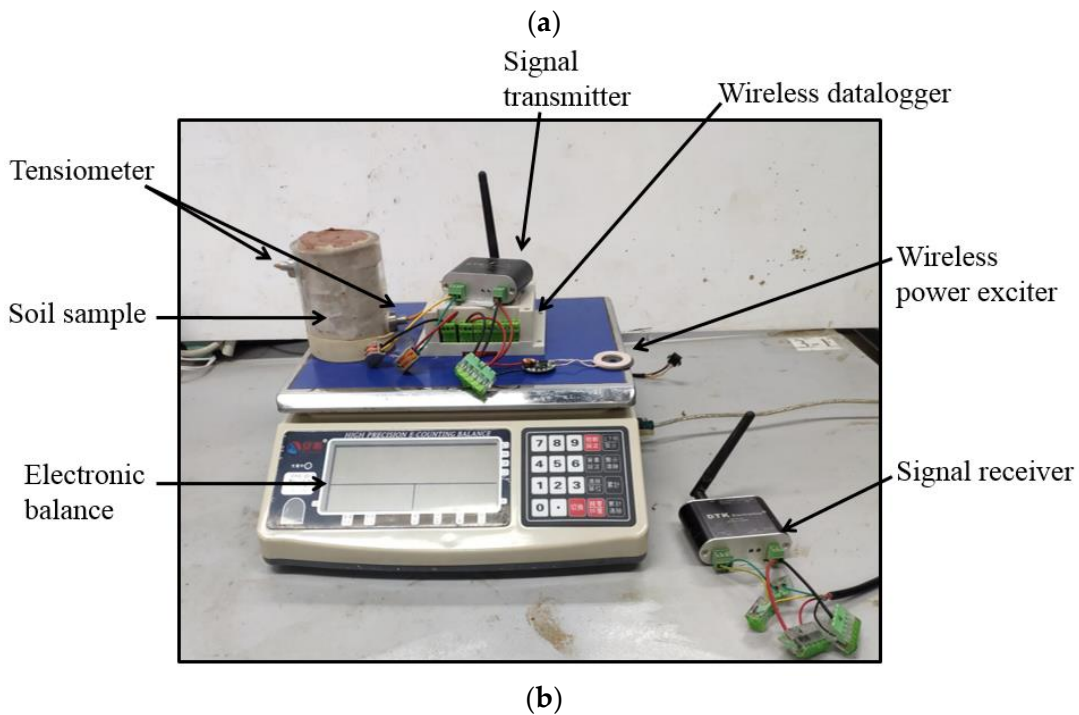
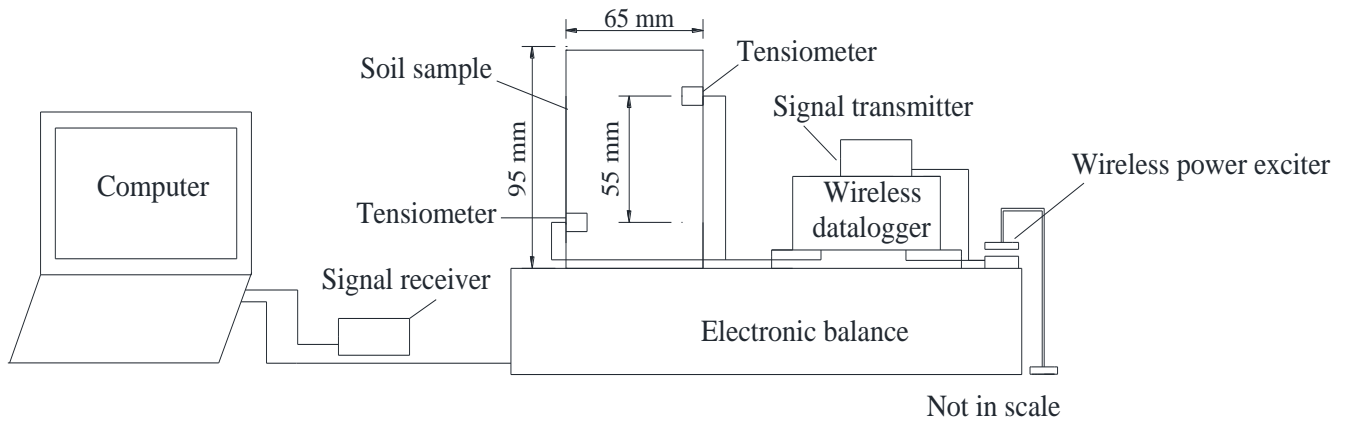


Figure 3. Testing setup for the evaporation tests: (a) schematic diagram; (b) photograph.

$$k(\bar{\psi}) = \frac{\Delta V}{2A \cdot \Delta t \cdot i_m} \tag{3}$$

$$i_m = \frac{1}{2} \left(\frac{\psi_{t1,upper} - \psi_{t1,lower}}{\Delta z} + \frac{\psi_{t2,upper} - \psi_{t2,lower}}{\Delta z} \right) - 1 \tag{4}$$

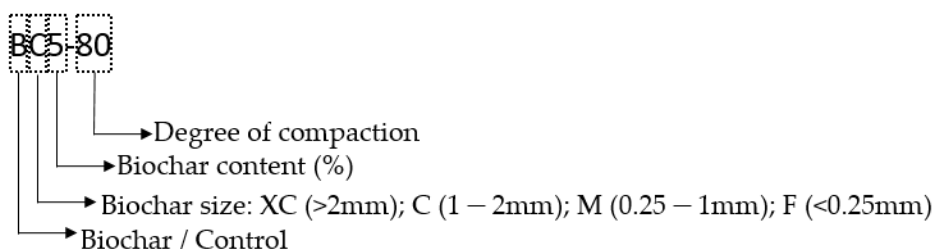
where $k(\bar{\psi})$ denotes the unsaturated permeability function of the BAS; $\bar{\psi}$ denotes the average suction measured by upper and lower tensiometer (kPa); ΔV is the volume of water loss in the soil sample during the time Δt (m^3); A is the cross-sectional area of the soil sample (m^2); i_m is the average hydraulic gradient; Δz is the vertical distance between upper and lower tensiometer (m); $\psi_{t,upper}$ denotes the suction measured by the upper tensiometer (kPa); and $\psi_{t,lower}$ denotes the suction measured by the lower tensiometer (kPa).

2.5. Test Program

A total of 34 soil specimens were employed in this study. Specifically, 17 of these specimens were dedicated to saturated permeability tests, while the remaining 17 specimens were prepared for evaporation tests. It is important to note that the preparation procedure for the 17 soil samples used in both the saturated permeability test and the evaporation experiments was identical. The experiments considered four different biochar particle sizes, namely, finer than 0.25 mm, 0.25–1 mm, 1–2 mm, and coarser than 2 mm, four biochar contents (0%, 5%, 10%, 20%), and two soil degrees of compaction (80% and 90%). The control for the experiments was soil without any biochar amendment. For the evaporation tests, the termination time was determined based on the range limit of the high capacity tensiometers used in the experiments, which was set at 500 kPa. Upon reaching readings of around 500 kPa, the evaporation tests were considered complete. The experimental program is summarized in Table 1.

Table 1. Test program.

Test ID	Biochar Particle Size (mm)	Biochar Content (%)	Degree of Compaction	Hydraulic Properties		
				Saturated Permeability	Soil Water Retention Curve	Unsaturated Permeability Function
C	-	0	80	/	/	/
BXC5-80	>2	5	80	/	/	/
BXC10-80		10		/	/	/
BXC20-80		20	/	/	/	
BXC10-90		10	90	/	/	/
BC5-80	1–2	5	80	/	/	/
BC10-80		10		/	/	/
BC20-80		20	/	/	/	
BC10-90		10	90	/	/	/
BM5-80	0.25–1	5	80	/	/	/
BM10-80		10		/	/	/
BM20-80		20	/	/	/	
BM10-90		10	90	/	/	/
BF5-80	<0.25	5	80	/	/	/
BF10-80		10		/	/	/
BF20-80		20	/	/	/	
BF10-90		10	90	/	/	/



3. Results and Discussion

3.1. Effects of Biochar Content on SWRC of BAS with Different Biochar Particle Sizes

Figure 4 presents the results of the measured SWRC of a compacted BAS system with varying biochar particle sizes and content levels. The degree of compaction was maintained at 90%. The results reveal that the impact of biochar on SWRC becomes increasingly pronounced as the biochar content increases. When the biochar content is low (i.e., 5%), the results indicate that the parameter “n” in the VG model is similar to that of bare soil, as indicated in Table 2. This parameter is one of the most important parameters in the model

and is used to describe the soil permeability and water-retention behavior. It is a measure of the soil's ability to store and release water and is related to the pore size distribution in the soil. This can be attributed to the fact that at low biochar content, the high porosity characteristics of the biochar are not fully developed; hence, its impact on the change in soil pore structure is minimal. However, as the biochar content increases, the saturated volumetric water content of the soil increases, indicating that the total porosity of the soil is augmented by the increased presence of biochar. When compared to the control group, it can be observed that the saturated volumetric water content significantly increases when biochar with particle sizes larger than 2 mm is added. These findings suggest that the addition of biochar to soil can significantly impact its water-holding capacity, and that this effect is influenced by the biochar content and particle size.

Table 2. VG model fitted parameters.

Soil Specimens	α (kPa)	n	m
0%	18.0	1.320	0.242
>2 mm (5%)	12.3	1.309	0.249
>2 mm (10%)	3.9	1.252	0.201
>2 mm (20%)	3.7	1.269	0.211
1–2 mm (5%)	6.9	1.270	0.212
1–2 mm (10%)	4.5	1.244	0.196
1–2 mm (20%)	3.5	1.289	0.224
0.25–1 mm (5%)	17.2	1.350	0.259
0.25–1 mm (10%)	8.7	1.241	0.192
0.25–1 mm (20%)	8.2	1.259	0.206
<0.25 mm (5%)	23.5	1.337	0.252
<0.25 mm (10%)	27.8	1.363	0.266
<0.25 mm (20%)	30.1	1.360	0.264

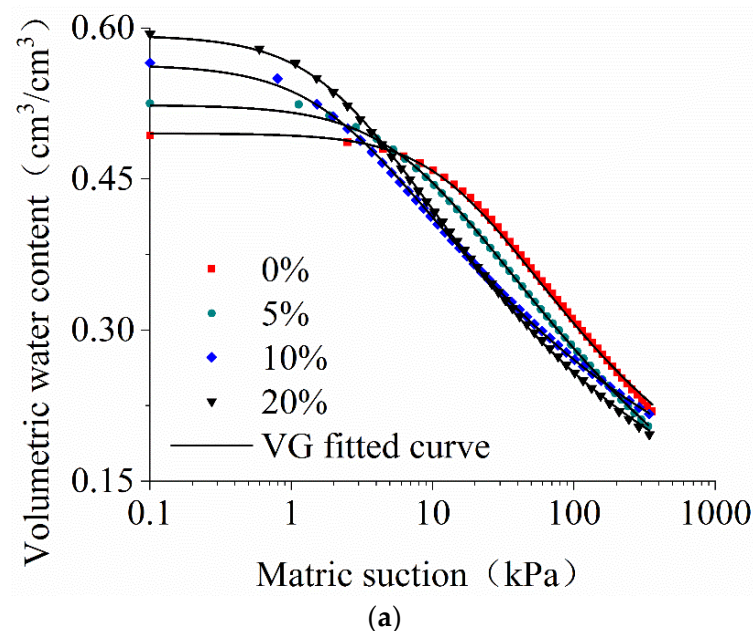


Figure 4. Cont.

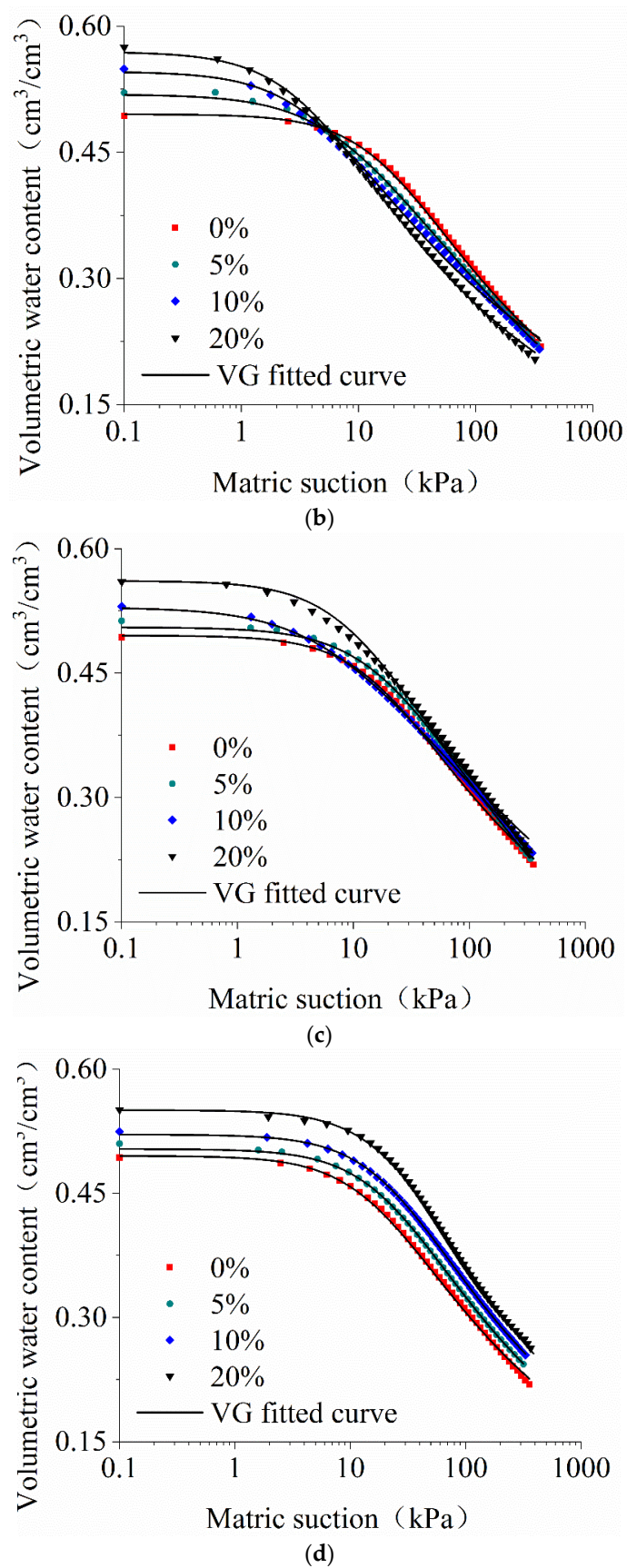


Figure 4. Effects of biochar content on SWRC of BAS at biochar particle size: (a) >2 mm; (b) 1–2 mm; (c) 0.25–1 mm; (d) <0.25 mm.

Figure 5 presents the correlation between the air entry value (AEV) of soil and the biochar content at various biochar particle sizes. It was observed that the AEV of soil decreased dramatically (from 18.0 kPa to 3.7 kPa) with the increase in large biochar particle content (coarser than 2 mm). This trend can be attributed to the fact that larger biochar particles increase the soil macropores [38,47], resulting in a decrease in AEV. Furthermore, the saturated volumetric water content for large biochar particle size (coarser than 2 mm) was lower compared to the control group, suggesting that the water-holding capacity of soil with coarse biochar was weaker at higher suction levels. The decrease in AEV after the addition of biochar was accompanied by a notable reduction in volumetric water content at low suction ranges (less than 100 kPa). This is most likely due to the influence of large biochar particles on soil pores, leading to a decline in the dehydration rate (parameter n) in the VG model for SWRCs. Moreover, the impacts of biochar particles ranging from 1–2 mm and larger than 2 mm on SWRC were similar. Conversely, the fine biochar particles (smaller than 0.25 mm), which were finer than the d_{55} particle size, significantly enhanced the soil's water holding capacity. It is noteworthy that particle size near soil grains has a strong impact on SWRC as it maximizes the contact surface area between the two. The water holding capacity of soil with fine biochar particles increased significantly with the increase in biochar content, and the AEV also increased (from 18.0 kPa to 30.1 kPa), indicating a reduction in soil macropores. Furthermore, the increase in biochar content led to an increase in the dehydration rate (parameter n) in the VG model (from 1.320 to 1.368). This can be attributed to the decrease in large pores in soil and the increase in small pores, resulting in higher air entry values and a faster dehumidification rate [44].

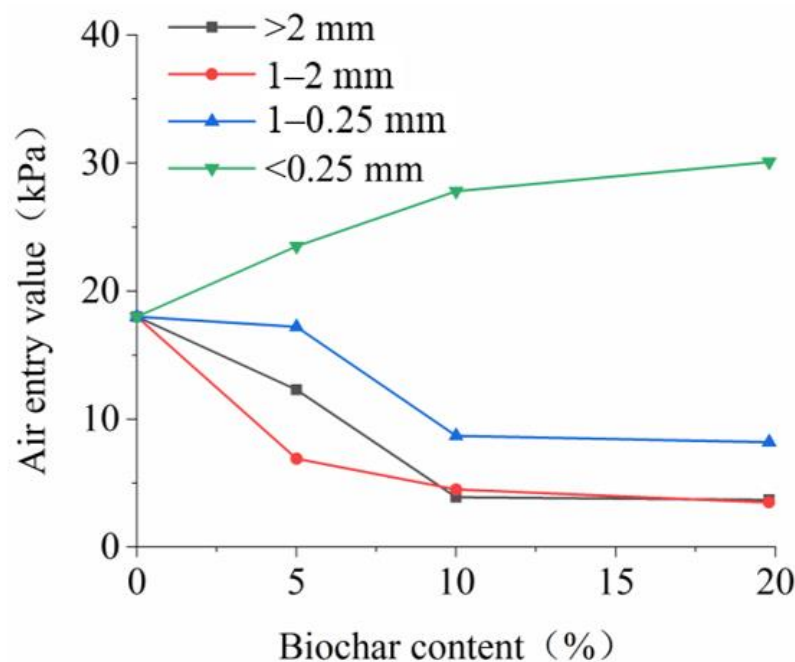


Figure 5. Effects of biochar content on air entry value of biochar amended CDG.

3.2. Effects of Biochar Content on the Unsaturated Permeability of BAS

Figure 6 displays the variation of the unsaturated permeability of the BAS soil at different levels of biochar content and particle size. The soil in this case has identical density and was compacted to 90% of its maximum density. As observed in Figure 6a, the permeability of soil is higher in the case of biochar particles coarser than 2 mm and lower matric suction (i.e., lower than 10 kPa) compared to the control group. This difference becomes more pronounced as the biochar content increased from 0–20%. This may be due to the increased macro-porosity of coarse biochar as compared with fine biochar [35]. Figure 6b displays a similar effect of biochar particle sizes of 1–2 mm on the unsaturated

permeability. However, as shown in Figure 6c, the addition of biochar particles sizes of 1–0.25 mm had little effect on the unsaturated permeability of BAS soil. This may be because these biochar particles are equivalent to the d_{70} to d_{55} size range of soil grain size, which was previously observed to have limited influence on the soil water retention capacity as indicated in Figure 4. In Figure 6d, it can be seen that with a low biochar content (5%), the impact of finer biochar particles (less than 0.25 mm) on the permeability is not significant. However, with an increase in biochar content, the permeability of soil decreases in the low suction range. At larger suction values, an increase in biochar content results in an increase in permeability. The observed reduction in soil permeability at low suction range in the presence of biochar may be due to an insufficient content of the biochar material. As the biochar content increases, the fine particles of the material fill the soil macro-pores, leading to a decrease in permeability. On the other hand, the soil permeability at high suction range is mainly controlled by the micro- and meso-pores [26]. The filling effect of fine biochar particles is less pronounced on the micro- and meso-pores at high suction, leading to an increase in permeability with increasing biochar content [35]. This indicates that incorporating larger amounts of finer biochar particles into the soil may help reduce the unsaturated permeability and enhance the soil's water holding capacity for biochar applications.

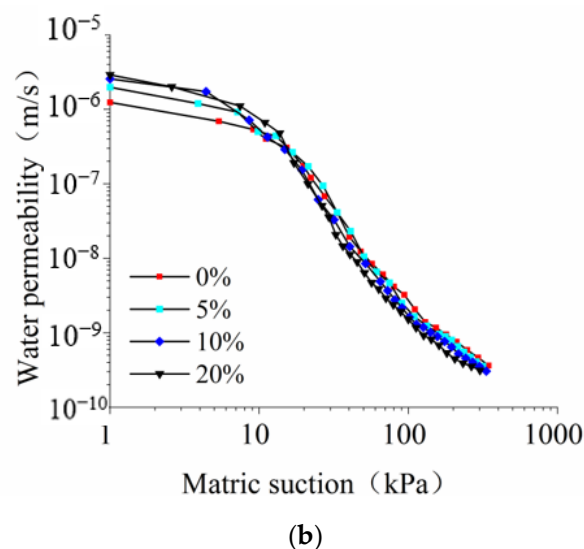
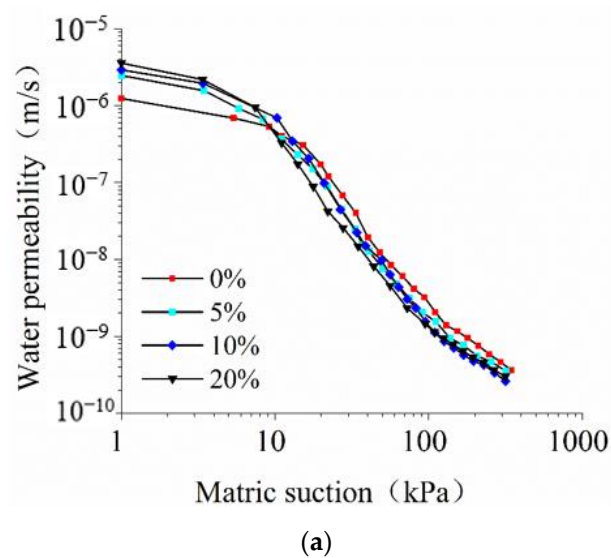
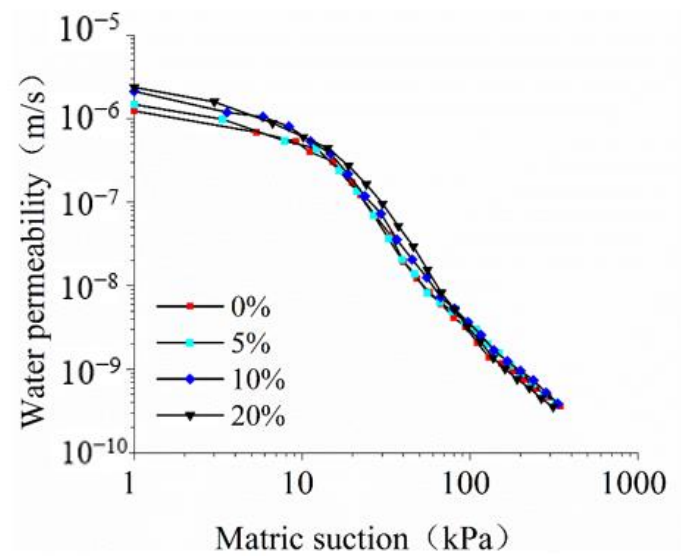
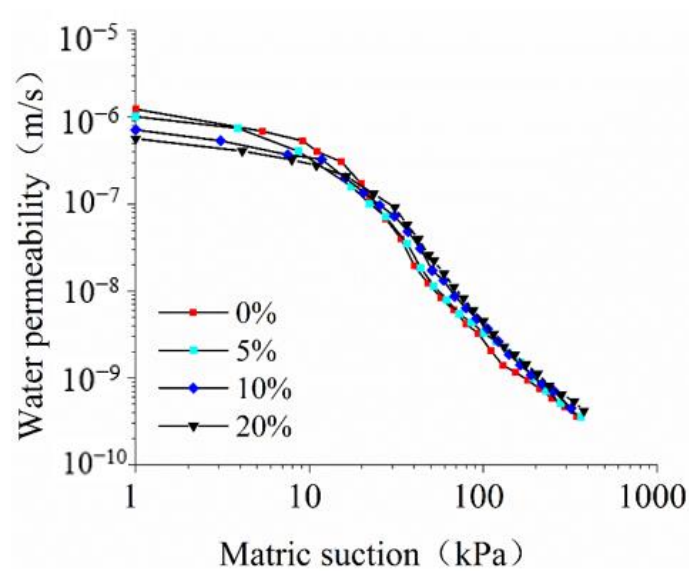


Figure 6. Cont.



(c)



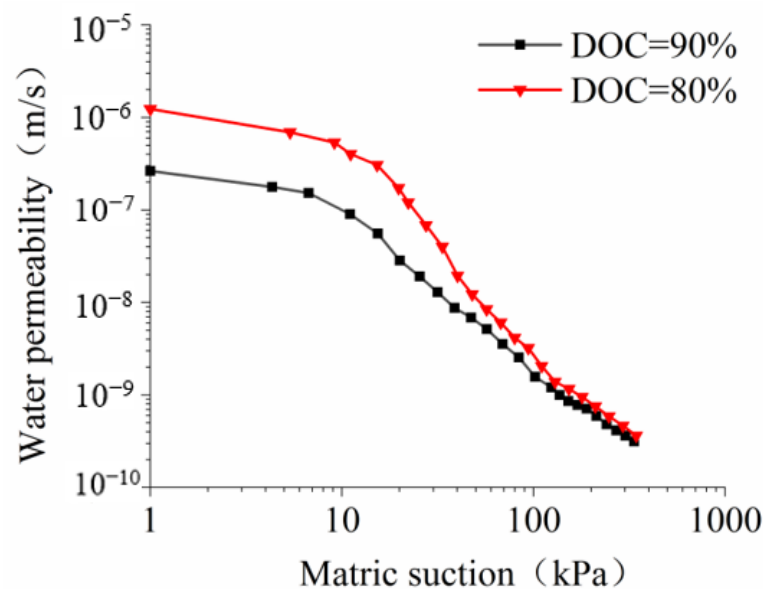
(d)

Figure 6. Effects of biochar content on the unsaturated water permeability of BAS at biochar particle size: (a) >2 mm; (b) 1–2 mm; (c) 0.25–1 mm; (d) <0.25 mm.

3.3. Effects of Degree of Compaction on the Unsaturated Permeability of BAS

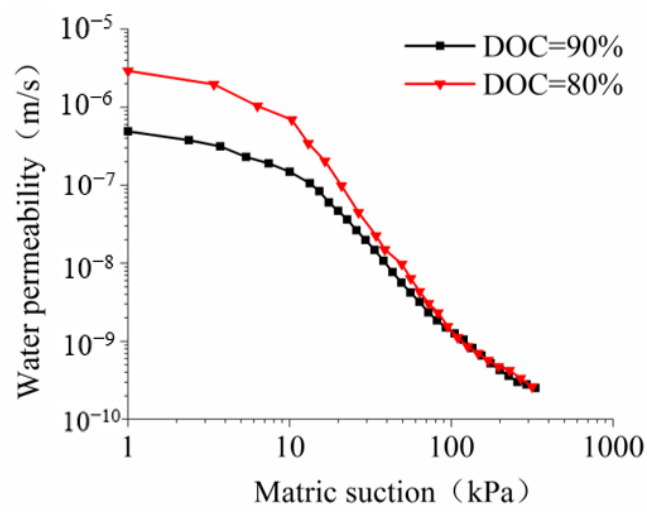
Figure 7 displays the unsaturated permeability function of BAS at two different degrees of compaction. As depicted in the figure, the effect of compaction on the unsaturated permeability of BAS with varying biochar particle sizes is similar. At low matric suction values, it can be observed that the unsaturated permeability of soil with 90% compaction decreases significantly. This is because with an increase in soil compaction, the diameter of soil pores decreases, resulting in less pore connectivity and a decrease in permeability. As the matric suction increases, the volumetric water content of soil with 80% compaction decreases, leading to a decrease in the water seepage cross-section and unsaturated water permeability coefficient. However, when the matric suction reaches around 100 kPa, the unsaturated permeability of soils with both compaction levels becomes similar. As the matric suction continues to increase beyond 100 kPa, the difference in unsaturated permeability between soils with different compaction levels is reduced. This is because

the compaction level primarily affects the number of large pores in the soil, while having little impact on the small pores. The water retention and permeability characteristics of soils at high matric suction are primarily determined by the small pores. The investigation of various factors, including biochar particle size, biochar content, and soil compaction, revealed significant effects on the water retention and permeability of the BAS. Specifically, when comparing fine biochar particles (<0.25 mm) to coarse biochar particles (>2 mm), the fine particles had a notable impact on improving water retention and reducing permeability, regardless of the biochar content and soil compaction degree. For instance, when examining the air entry value (α) in Table 2, we observed that BAS with a biochar particle size of <0.25 mm at 20% biochar content had a significantly higher α value (30.1 kPa) compared to BAS with a biochar particle size of >2 mm ($\alpha = 3.7$ kPa). This indicates that the finer biochar particles greatly enhanced the soil's ability to retain water. The study by Chen et al. [35] also aligns with these findings, as they reported that an increase in biochar particle size (specifically peanut shell biochar) led to an increase in biochar pore size. In general, the addition of coarse biochar particles (>2 mm) to the soil resulted in an increase in macropores and a decrease in micropores in the silty sand. Furthermore, the biochar content also had a similar impact on the air entry value of the BAS compared to the biochar particles size. However, the influence of biochar content on unsaturated permeability was not significant across different biochar particle sizes, particularly at high suction ranges. Regardless of the biochar particle size and biochar content, we found that increasing the degree of compaction from 80% to 90% resulted in a significant reduction in soil permeability. This reduction in permeability highlights the importance of soil compaction in controlling the movement of water, regardless of other factors. Therefore, when manipulating the unsaturated hydraulic properties of BAS, it is essential to pay close attention to the low suction range, which is typically more sensitive to the performance of geo-environmental systems such as landfill covers and slopes. This sensitivity is often attributed to the high water content that is present in this range.

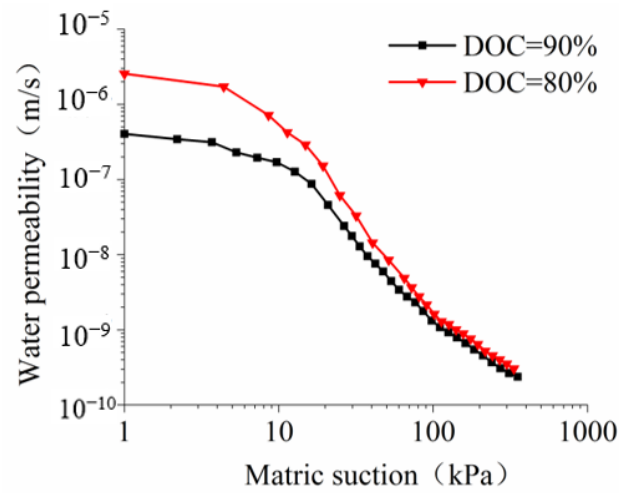


(a)

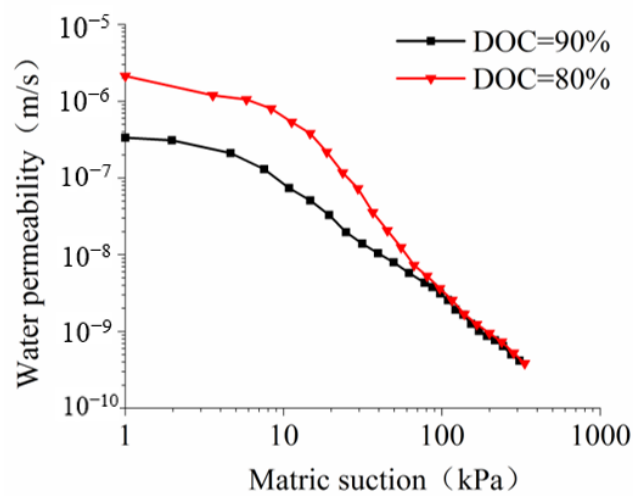
Figure 7. Cont.



(b)

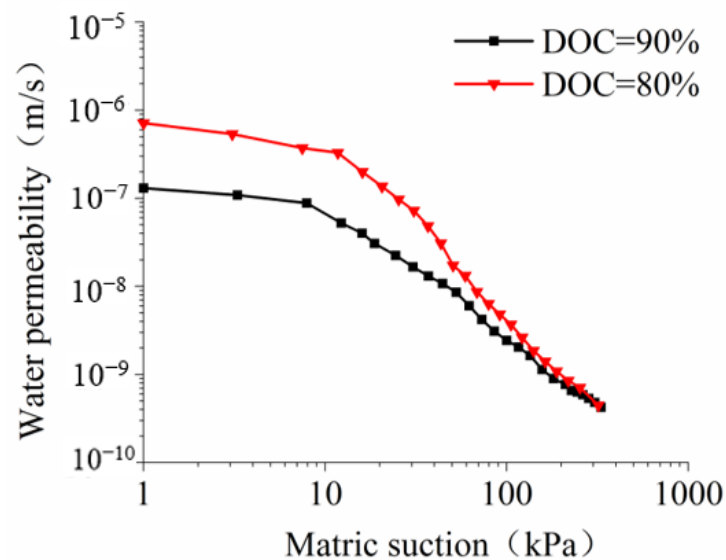


(c)



(d)

Figure 7. Cont.



(e)

Figure 7. Effects of degree of compaction (DOC) on the unsaturated water permeability of BAS (10% biochar content) at biochar particle size: (a) CDG; (b) >2 mm; (c) 1–2 mm; (d) 0.25–1 mm; (e) <0.25 mm.

3.4. Effects of Degree of Compaction on Saturated Water Permeability of BAS

Figure 8 displays the saturation permeability of BAS with various particle sizes of biochar at two levels of compaction: 80% and 90%. The results indicate that the saturation permeability of BAS decreases significantly with an increase in the compaction degree from 80% to 90% for all the biochar particle size groups. This observation is in accordance with the findings reported by Imhoff et al. [48]. This is because the increase in compaction degree can result in the reduction in pore volume and connected macropores in the soil mass. In comparison to the control group, the saturation permeability decreases for biochar particle size finer than 0.25 mm at both 80% and 90% compaction degrees. However, it increases for the three other particle size groups (0.25–1 mm, 1–2 mm, and coarser than 2 mm). The reduction in the particle size of biochar has been shown to decrease the permeability of BAS due to the pore-filling effect observed in previous studies (e.g., Wan et al. [49]). However, as the particle size of biochar increases and approaches a certain range (i.e., 0.25 mm as demonstrated in this study), the pore-filling effect may become weaker or diminished due to the relative comparison of the biochar particle size to that of the soil grain size [39]. In situations where the biochar particle size is larger than the soil grain size, the soil macropores are increased, leading to an increase in permeability. Furthermore, the saturation permeability of BAS increases with an increase in the biochar particle size. At 90% compaction, the increment of saturation permeability is reduced for the coarse biochar particle sizes (0.25–1 mm: 89%→27%; 1–2 mm: 107%→54%; coarser than 2 mm: 135%→85%) compared to 80% compaction. This reduction may be due to the reduction in the influence of coarse biochar on the soil's macropores and the reduction in particle size of biochar due to its fragmentation under high compaction [50]. Bronick et al. [51] also suggested that soil compaction might result in different pore structures in soil and reduced macropores. Therefore, both reducing the particle size of biochar and increasing the compaction degree can decrease the soil's saturation permeability.

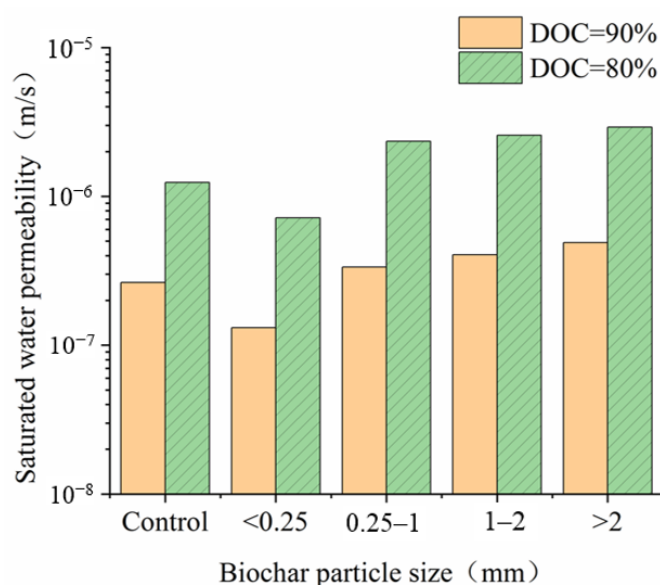


Figure 8. Effects of degree of compaction (DOC) on saturated water permeability of BAS.

4. Conclusions

This study aimed to explore the water retention behavior and permeability of BAS under different biochar contents and compaction levels. Through a series of evaporation tests and falling head tests, the following conclusions were drawn:

1. Biochar addition significantly influenced the water retention properties of the soil, particularly at low suction range. Increasing biochar content resulted in higher saturated volumetric water content, indicating an increase in total porosity. Fine biochar particles (finer than 0.25 mm) enhanced the soil's water holding capacity and increased the air entry value (AEV) of the soil.
2. The addition of biochar had a notable impact on the saturated and unsaturated permeability of the soil. Saturated permeability decreased with higher biochar content and degree of compaction. However, the relationship between biochar content and unsaturated permeability was more intricate, with a decrease observed at low soil suction values and an increase at high soil suction values. This suggests that the effect of biochar on permeability is dependent on soil water content.
3. Among the soil groups investigated in this study, the combination of biochar particle size < 0.25 mm and a biochar content of 20% demonstrated the most suitable characteristics for reducing soil permeability and enhancing soil water retention.

The findings of this study have practical implications for two main applications. In agriculture, incorporating biochar into soil amendment practices can enhance water retention capacity, benefiting regions prone to drought. The addition of biochar, especially fine particles, improves the soil's water-holding ability, supporting optimal plant growth and resilience in water-limited conditions. In geoen지니어ing, understanding the impact of biochar on soil permeability is crucial for designing effective landfill covers and erosion control measures. Engineers can develop sustainable solutions by considering compaction levels and biochar content to minimize water percolation and enhance the stability of embankments and slopes. Further research is necessary to investigate the intricate interactions among biochar, soil compaction, and water dynamics, enabling the development of tailored and sustainable biochar applications that improve agriculture practices and foster more resilient geoen지니어ing systems.

Author Contributions: Conceptualization, Z.C.; Data curation, L.P.; Formal analysis, Z.C. and R.C.; Funding acquisition, Z.C. and V.K.; Investigation, Z.C., R.C., and V.K.; Methodology, Z.C., R.C. and V.K.; Visualization, L.P.; Writing—original draft, Z.C.; Writing—review and editing, V.K., R.C. and L.P. All authors have read and agreed to the published version of the manuscript.

Funding: This research was funded by the National Natural Science Foundation of China [No. 51808171], the King Mongkut's Institute of Technology Ladkrabang (KMITL) and National Science, Research and Innovation Fund (NSRF) [No. FRB66065/0258-RE-KRIS/FF66/53], and Climate Change and Climate Variability Research in Monsoon Asia (CMON3) from the National Research Council of Thailand (NRCT) and the National Natural Science Foundation of China (NSFC) [No. N10A650844].

Data Availability Statement: Not applicable.

Conflicts of Interest: The authors declare no conflict of interest.

References

- Lehmann, J.; Joseph, S. Biochar for environmental management: An introduction. In *Biochar for Environmental Management: Science and Technology*; Lehmann, J., Joseph, S., Eds.; Earthscan: London, UK, 2009. [[CrossRef](#)]
- Liu, H.; Kumar, V.; Yadav, V.; Guo, S.; Sarsaiya, S.; Binod, P.; Sindhu, R.; Xu, P.; Zhang, Z.; Pandey, A.; et al. Bioengineered biochar as smart candidate for resource recovery toward circular bio-economy: A review. *Bioengineered* **2021**, *12*, 10269–10301. [[CrossRef](#)]
- Lehmann, J.; Cowie, A.; Masiello, C.A.; Kammann, C.; Woolf, D.; Amonette, J.E.; Cayuela, M.L.; Arbestain, M.C.; Whitman, T. Biochar in climate change mitigation. *Nat. Geosci.* **2021**, *14*, 883–892. [[CrossRef](#)]
- Yang, W.; Feng, G.; Miles, D.; Gao, L.; Jia, Y.; Li, C.; Qu, Z. Impact of biochar on greenhouse gas emissions and soil carbon sequestration in corn grown under drip irrigation with mulching. *Sci. Total Environ.* **2020**, *729*, 138752. [[CrossRef](#)]
- Tripathi, M.; Sahu, J.; Ganesan, P. Effect of process parameters on production of biochar from biomass waste through pyrolysis: A review. *Renew. Sustain. Energy Rev.* **2016**, *55*, 467–481. [[CrossRef](#)]
- Jeffery, S.; Verheijen, F.G.A.; Kammann, C.; Abalos, D. Biochar effects on methane emissions from soils: A meta-analysis. *Soil Biol. Biochem.* **2016**, *101*, 251–258. [[CrossRef](#)]
- Garg, A.; Bordoloi, S.; Ni, J.; Cai, W.; Maddibiona, P.G.; Mei, G.; Poulsen, T.G.; Lin, P. Influence of biochar addition on gas permeability in unsaturated soil. *Geotech. Lett.* **2019**, *9*, 66–71. [[CrossRef](#)]
- Leng, L.; Xiong, Q.; Yang, L.; Li, H.; Zhou, Y.; Zhang, W.; Jiang, S.; Li, H.; Huang, H. An overview on engineering the surface area and porosity of biochar. *Sci. Total Environ.* **2021**, *763*, 144204. [[CrossRef](#)] [[PubMed](#)]
- Katiyar, R.; Chen, C.-W.; Singhania, R.R.; Tsai, M.-L.; Saratale, G.D.; Pandey, A.; Dong, C.-D.; Patel, A.K. Efficient remediation of antibiotic pollutants from the environment by innovative biochar: Current updates and prospects. *Bioengineered* **2022**, *13*, 14730–14748. [[CrossRef](#)] [[PubMed](#)]
- Garg, A.; Huang, H.; Cai, W.; Reddy, N.G.; Chen, P.; Han, Y.; Kamchoom, V.; Gaurav, S.; Zhu, H.-H. Influence of soil density on gas permeability and water retention in soils amended with in-house produced biochar. *J. Rock Mech. Geotech.* **2021**, *13*, 593–602. [[CrossRef](#)]
- Chen, Z.; Kamchoom, V.; Chen, R. Landfill gas emission through compacted clay considering effects of crack pathway and intensity. *Waste Manag.* **2022**, *143*, 215–222. [[CrossRef](#)]
- Bohnert, H.J.; Jensen, R.G. Strategies for engineering water-stress tolerance in plants. *Trends Biotechnol.* **1996**, *14*, 89–97. [[CrossRef](#)]
- Shao, H.-B.; Chu, L.-Y.; Lu, Z.-H.; Kang, C.-M. Primary antioxidant free radical scavenging and redox signaling pathways in higher plant cells. *Int. J. Biol. Sci.* **2007**, *4*, 8–14. [[CrossRef](#)] [[PubMed](#)]
- Apriyono, A.; Yuliana; Kamchoom, V. Serviceability of cut slope and embankment under seasonal climate variations. *Acta Geophys.* **2023**, *71*, 983–995. [[CrossRef](#)]
- Lu, J.-H.; Chen, C.; Huang, C.; Lee, D.-J. Glucose fermentation with biochar-amended consortium: Microbial consortium shift. *Bioengineered* **2020**, *11*, 272–280. [[CrossRef](#)] [[PubMed](#)]
- Hossain, M.Z.; Bahar, M.M.; Sarkar, B.; Donne, S.W.; Ok, Y.S.; Palansooriya, K.N.; Kirkham, M.B.; Chowdhury, S.; Bolan, N. Biochar and its importance on nutrient dynamics in soil and plant. *Biochar* **2020**, *2*, 379–420. [[CrossRef](#)]
- Treebupachatsakul, T.; Kamchoom, V. Permeability and setting time of bio-mediated soil under various medium concentrations. *J. Rock Mech. Geotech. Eng.* **2021**, *13*, 401–409. [[CrossRef](#)]
- Barnes, R.T.; Gallagher, M.E.; Masiello, C.A.; Liu, Z.; Dugan, B. Biochar-induced changes in soil hydraulic conductivity and dissolved nutrient fluxes constrained by laboratory experiments. *PLoS ONE* **2014**, *9*, e108340. [[CrossRef](#)]
- Lim, T.J.; Spokas, K.A.; Feyereisen, G.; Novak, J.M. Predicting the impact of biochar additions on soil hydraulic properties. *Chemosphere* **2016**, *142*, 136–144. [[CrossRef](#)]
- Sun, F.F.; Lu, S.G. Biochars improve aggregate stability, water retention, and pore-space properties of clayey soil. *J. Plant Nutr. Soil Sci.* **2013**, *177*, 26–33. [[CrossRef](#)]
- Głab, T.; Palmowska, J.; Zaleski, T.; Gondek, K. Effect of biochar application on soil hydrological properties and physical quality of sandy soil. *Geoderma* **2016**, *281*, 11–20. [[CrossRef](#)]

22. Wong, J.T.F.; Chen, Z.; Chen, X.; Ng, C.W.W.; Wong, M.H. Soil-water retention behavior of compacted biochar-amended clay: A novel landfill final cover material. *J. Soils Sediments* **2017**, *17*, 590–598. [[CrossRef](#)]
23. Omondi, M.O.; Xia, X.; Nahayo, A.; Liu, X.; Korai, P.K.; Pan, G. Quantification of biochar effects on soil hydrological properties using meta-analysis of literature data. *Geoderma* **2016**, *274*, 28–34. [[CrossRef](#)]
24. Edeh, I.G.; Mašek, O.; Buss, W. A meta-analysis on biochar's effects on soil water properties—New insights and future research challenges. *Sci. Total Environ.* **2020**, *714*, 136857. [[CrossRef](#)]
25. Ng, C.W.W.; Menzies, B. *Advanced Unsaturated Soil Mechanics and Engineering*; Taylor & Francis: London, UK; New York, NY, USA, 2007; ISBN 978-0-415-43679-3.
26. Fredlund, D.G.; Rahardjo, H.; Fredlund, M.D. *Unsaturated Soil Mechanics in Engineering Practice*; John Wiley & Sons, Inc.: Hoboken, NJ, USA, 2012.
27. Brantley, K.E.; Brye, K.R.; Savin, M.C.; Longer, D.E. Biochar source and application rate effects on soil water retention determined using wetting curves. *Open J. Soil Sci.* **2015**, *5*, 51001. [[CrossRef](#)]
28. Trifunovic, B.; Gonzales, H.B.; Ravi, S.; Sharratt, B.S.; Mohanty, S.K. Dynamic effects of biochar concentration and particle size on hydraulic properties of sand. *Land Degrad. Dev.* **2018**, *29*, 884–893. [[CrossRef](#)]
29. Leung, A.K.; Kamchoom, V.; Ng, C.W.W. Influences of root-induced soil suction and root geometry on slope stability: A centrifuge study. *Can. Geotech. J.* **2017**, *54*, 291–303. [[CrossRef](#)]
30. Ng, C.W.W.; Leung, A.K.; Yu, R.; Kamchoom, V. Hydrological effects of live poles on transient seepage in an unsaturated soil slope: Centrifuge and numerical study. *J. Geotech. Geoenviron. Eng. ASCE* **2017**, *143*, 04016106. [[CrossRef](#)]
31. Kamchoom, V.; Leung, A.K. Hydro-mechanical reinforcements of live poles to slope stability. *Soils Found.* **2018**, *58*, 1423–1434. [[CrossRef](#)]
32. Chen, Z.K.; Kamchoom, V.; Apriyono, A.; Chen, R.; Chen, C.W. Laboratory study of water infiltration and evaporation in biochar-amended landfill covers under extreme climate. *Waste Manag.* **2022**, *153*, 323–334. [[CrossRef](#)]
33. Hussain, R.; Ravi, K.; Garg, A. Influence of biochar on the soil water retention characteristics (SWRC): Potential application in geotechnical engineering structures. *Soil Tillage Res.* **2020**, *204*, 104713. [[CrossRef](#)]
34. Ng, C.W.W.; Chen, Z.K.; Co, J.L.; Chen, R.; Zhou, C. Gas breakthrough and emission through unsaturated compacted clay in landfill final cover. *Waste Manag.* **2015**, *44*, 155–163. [[CrossRef](#)] [[PubMed](#)]
35. Chen, Z.; Chen, C.; Kamchoom, V.; Chen, R. Gas permeability and water retention of a repacked silty sand amended with different particle sizes of peanut shell biochar. *Soil Sci. Soc. Am. J.* **2020**, *84*, 1630–1641. [[CrossRef](#)]
36. Ding, Y.; Liu, Y.; Liu, S.; Li, Z.; Tan, X.; Huang, X.; Zeng, G.; Zhou, L.; Zheng, B. Biochar to improve soil fertility. A review. *Agron. Sustain. Dev.* **2016**, *36*, 36. [[CrossRef](#)]
37. Strunecký, O.; Shreedhar, S.; Kolář, L.; Maroušková, A. Changes in soil water retention following biochar amendment. In *Energy Sources, Part A: Recovery, Utilization, and Environmental Effects*; Taylor & Francis: London, UK; New York, NY, USA, 2021. [[CrossRef](#)]
38. Alghamdi, A.G.; Alkhasha, A.; Ibrahim, H.M. Effect of biochar particle size on water retention and availability in a sandy loam soil. *J. Saudi Chem. Soc.* **2020**, *24*, 1042–1050. [[CrossRef](#)]
39. Liu, Z.; Dugan, B.; Masiello, C.A.; Gonnermann, H.M. Biochar particle size, shape, and porosity act together to influence soil water properties. *PLoS ONE* **2017**, *12*, e0179079. [[CrossRef](#)] [[PubMed](#)]
40. Zheng, Q.-F.; Wang, Y.-H.; Sun, Y.-G.; Niu, H.-H.; Zhou, J.-R.; Wang, Z.-M.; Zhao, J. Study on structural properties of biochar under different materials and carbonized by FTIR. *Spectrosc. Spectr. Anal.* **2014**, *34*, 962–966.
41. *ASTM C1202*; Standard Test Method for Electrical Indication of Concrete's Ability to Resist Chloride Ion Penetration. American Society for Testing Materials: West Conshohocken, PA, USA, 2006.
42. *ISO 17892-11:2019*; Geotechnical Investigation and Testing—Laboratory Testing of Soil—Part 11: Permeability Tests. ISO: Geneva, Switzerland, 2019.
43. Schindler, U.; Müller, L. Simplifying the evaporation method for quantifying soil hydraulic properties. *J. Plant Nutr. Soil Sci.* **2006**, *169*, 623–629. [[CrossRef](#)]
44. Chen, R.; Huang, J.W.; Chen, Z.K.; Xu, Y.; Liu, J.; Ge, Y.H. Effect of root density of wheat and okra on hydraulic properties of an unsaturated compacted loam. *Eur. J. Soil Sci.* **2019**, *70*, 493–506. [[CrossRef](#)]
45. Chen, R.; Liu, J.; Li, J.H.; Ng, C.W.W. An integrated high-capacity tensiometer for measuring water retention curves continuously. *Soil Sci. Soc. Am. J.* **2015**, *79*, 943–947. [[CrossRef](#)]
46. van Genuchten, M.T. A closed-form equation for predicting the hydraulic conductivity of unsaturated soils. *Soil Sci. Soc. Am. J.* **1980**, *44*, 892–898. [[CrossRef](#)]
47. Edeh, I.G.; Mašek, O. The role of biochar particle size and hydrophobicity in improving soil hydraulic properties. *Eur. J. Soil Sci.* **2021**, *73*, e13138. [[CrossRef](#)]
48. Imhoff, P.T.; Nakhli, S.A.A. Reducing stormwater runoff and pollutant loading with biochar addition to highway greenways. *No. Nchrp. Idea Proj.* **2017**, *182*, 7–22.
49. Wan, Y.; Dong, Z.; He, X.; Liu, R.; Cai, Y.; Liu, L.; Qin, L.; Xue, Q. Effect of biochar on permeability of compacted soil and its microscopic mechanism. *Can. Geotech. J.* **2022**, *59*, 2184–2195. [[CrossRef](#)]

50. Spokas, K.A.; Novak, J.M.; Masiello, C.A.; Johnson, M.G.; Colosky, E.C.; Ippolito, J.A.; Trigo, C. Physical disintegration of biochar: An overlooked process. *Environ. Sci. Technol. Lett.* **2014**, *1*, 326–332. [[CrossRef](#)]
51. Bronick, C.J.; Lal, R. Soil structure and management: A review. *Geoderma* **2005**, *124*, 3–22. [[CrossRef](#)]

Disclaimer/Publisher’s Note: The statements, opinions and data contained in all publications are solely those of the individual author(s) and contributor(s) and not of MDPI and/or the editor(s). MDPI and/or the editor(s) disclaim responsibility for any injury to people or property resulting from any ideas, methods, instructions or products referred to in the content.